

Resonant Rayleigh scattering from a disordered microcavity

D. M. Whittaker

Toshiba Research Europe Limited, 260 Cambridge Science Park, Cambridge CB4 0WE, United Kingdom

(Received 23 September 1999; revised manuscript received 9 November 1999)

The problem of Rayleigh scattering from a microcavity containing a disordered quantum well is treated both analytically and numerically. The results show that the effect of the microcavity is to act as a filter for the Rayleigh scattering which occurs in the quantum well. This simple model works because multiple scattering between microcavity polariton modes is strongly suppressed due to their low density of states.

Over the last few years, an understanding of how quantum well disorder affects the line widths in microcavity reflectivity spectra has been developed.¹⁻⁶ The model which is now established, theoretically⁵ and experimentally,⁶ includes disorder scattering of the exciton to all orders, producing a broadened distribution of optically active exciton states,^{1,2} but neglects scattering between polariton modes with different wave vectors. This approximation has been described as the linear dispersion model.⁶ It works because the low momentum polaritons have an effective mass $m_p \sim 10^{-5} m_e$, so their density of states (DOS) is very small, which effectively suppresses scattering between polariton modes.^{3,4} As a result, reflectivity line widths are determined by scattering from the optically excited polariton modes to the much larger DOS of effectively uncoupled high momentum exciton states. It is only in structures with very small exciton line widths, where there are no exciton states resonant with the polariton features, that scattering between polariton modes becomes important. However, in this limit the quantum well disorder contribution to the reflectivity line widths, estimated as $\sim 10^{-4}$ meV,⁵ is negligible compared to the homogeneous broadening, ≥ 0.1 meV, due to the finite cavity photon lifetime.

The linear dispersion model of microcavity disorder appears to be completely adequate to describe reflectivity line widths in present day microcavity structures. However, the effects of disorder are probed more directly by another type of experiment, resonant Rayleigh scattering (RRS).⁷ RRS involves the detection of photons scattered into directions other than that of the specular reflection, a process which requires the presence of disorder. Thus microcavity RRS (MC-RRS) measures the scattering between polariton modes with different wave vectors, which necessitates a treatment beyond the linear dispersion model. The theoretical results presented in this paper show that MC-RRS is well described by a model which includes disorder scattering of the exciton to all orders, but involves only a single scattering between polariton modes. This approximation works because, once again, scattering between polariton modes is strongly suppressed by their low DOS. Of course, unlike in specular reflectivity, a single scattering has to be included to describe the change in wave vector involved in a RRS measurement. A consequence of being able to neglect multiple scattering is that, in the frequency domain, the microcavity acts as a simple filter, controlling the strength of the contribution of the quantum well RRS (QW-RRS) signal at a particular en-

ergy. The filter function can be determined using parameters obtained from measurements of specular reflectivity spectra.

The filter model of MC-RRS described in the previous paragraph can be expressed more formally in terms of the exciton and polariton Green's functions. Figure 1 shows diagrammatically how the off-diagonal polariton Green's function is built up. The interaction between the exciton and the quantum well disorder potential is fully described by the diagonal, $G_e(k; \omega)$, and off-diagonal, $G_e(k, k'; \omega)$ exciton propagators, which include scattering by the disorder potential to all orders. The diagonal polariton propagator, $G_p(k; \omega)$, includes only diagonal exciton terms, so the photon wave vector is conserved. This approximation leads to the linear dispersion model for the polariton.⁵ The filter model of MC-RRS is obtained by including in the off-diagonal polariton propagator, $G_p(k, k'; \omega)$, just one diagram, which contains only a single change in photon wave vector. All other contributions involve two or more changes in polariton wave vector, and so are strongly suppressed for the reasons discussed above.

It is now possible to make clearer the previously rather arbitrary distinction between exciton and polariton scattering: polariton scattering requires a change in the wave vector of the photon part. Thus the approximation to $G_p(k; \omega)$ does not involve any changes in polariton wave vector, even though it is made from $G_e(k; \omega)$, which describes exciton scattering to all orders.

The diagrams of Fig. 1 are readily summed to give ap-

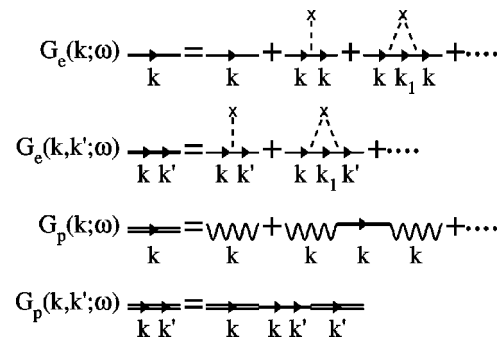


FIG. 1. The hierarchy of Green's functions describing the filter model of microcavity resonant Rayleigh scattering. $G_e(k, k'; \omega)$ is the bare exciton propagator, including its interaction with the quantum well disorder potential. $G_p(k, k'; \omega)$ is the polariton propagator, which accounts for the exciton-photon interaction to all orders, but only the lowest order scattering between polariton modes of different wave vectors.

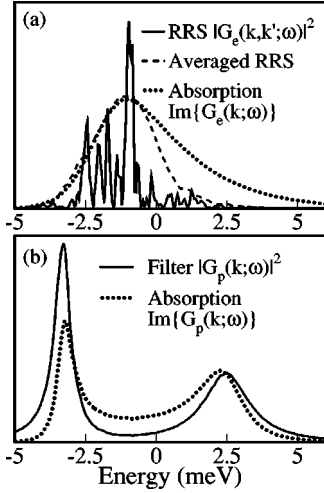


FIG. 2. (a) Typical quantum well resonant Rayleigh scattering spectrum, showing the effects of speckle. Also plotted are the smoothed configuration averaged Rayleigh spectrum, and, for comparison, the exciton absorption spectrum. (b) The microcavity filter function, and the corresponding absorption spectrum. The calculation is for a Gaussian correlated disorder potential with amplitude $V_0 = 5.0$ meV, and correlation length $l_c = 100$ Å. The exciton mass is $M_e = 0.25m_e$ and a homogeneous broadening of $\hbar\gamma = 0.1$ meV is used. The vacuum Rabi splitting is $\hbar\Omega = 5.0$ meV, and the cavity detuning is chosen to put the cavity and exciton on resonance ($\delta_k = 0$) for the incident angle of 24° . In the RRS calculation, the detection direction is at the same angle to the normal, but differs in azimuthal angle by 28° .

proximations to the diagonal⁵ and off-diagonal microcavity polariton Green's functions

$$G_p(k, \omega) = \frac{1}{\hbar\omega + i\hbar\gamma - \delta_k - (\hbar\Omega/2)^2 G_e(k; \omega)} \quad (1)$$

and

$$G_p(k, k'; \omega) = G_p(k; \omega) G_e(k, k'; \omega) G_p(k'; \omega). \quad (2)$$

Here γ is the photon homogeneous width, $\hbar\Omega$ the vacuum Rabi splitting energy, and δ_k the detuning for wave vector k .

The amplitude of the RRS signal at energy $\hbar\omega$ is proportional to $G(k, k'; \omega)$ where k, k' are the in-plane wave vectors corresponding to the excitation and detection directions.⁸ Hence the MC-RRS spectrum, $I_p(k, k'; \omega)$ is given by

$$\begin{aligned} I_p(k, k'; \omega) &\propto |G_p(k; \omega)|^2 |G_e(k, k'; \omega)|^2 |G_p(k'; \omega)|^2 \\ &= |G_p(k; \omega)|^2 I_e(k, k'; \omega) |G_p(k'; \omega)|^2, \end{aligned} \quad (3)$$

where $I_e(k, k'; \omega) \propto |G_e(k, k'; \omega)|^2$ is the QW-RRS spectrum.

Figure 2(a) shows a typical example of I_e , obtained from the numerical simulations discussed below. It is strongly dependent on the particular disorder potential in the calculation, which determines the details of the speckle apparent in the spectrum. The speckle is an interference effect, a result of the random phases of the Rayleigh signal from the various areas of the structure which contribute significantly at a given frequency.

To obtain the MC-RRS spectrum, I_p , the QW-RRS spectrum is multiplied by the functions $|G_p(k; \omega)|^2$, $|G_p(k'; \omega)|^2$

describing the filtering effect of the cavity for the excitation and detection directions. $|G_p(k; \omega)|^2$ is related to the microcavity absorption spectrum which is proportional to $\text{Im}\{G_p(k; \omega)\}$. Unlike I_e , in the limit of large system size it is a smooth function,⁹ independent of the microscopic details of the disorder potential, so it is justified to describe its effect as simply filtering the underlying QW-RRS spectrum. Figure 2(b) shows the calculated filter function $|G_p(k; \omega)|^2$, for the same disorder potential as Fig. 2(a), comparing it to the absorption spectrum $\text{Im}\{G_p(k; \omega)\}$. Although both curves are peaked at the polariton energies, the ratio of the strengths of the peaks is not the same for the two functions—the lower energy, narrower peak is more enhanced in the filter than in the absorption spectrum. More precisely, $G_p(k; \omega)$ looks approximately like the sum of two Lorentzian features, so in the vicinity of a peak, $\text{Im}\{G\} \approx (\Gamma/f)|G|^2$, where f and Γ are the strength and width of the corresponding Lorentzian.

Equation (3) shows that in order to observe strong MC-RRS, it is necessary to find an energy matching a polariton feature in both excitation and detection directions, so that the overlap of the filter spectra is significant. This is most easily achieved by choosing k and k' to have the same magnitude but different directions—that is, the same angle to the surface normal, but different azimuthal angles. Then the input and output filter functions are the same, so their overlap is maximized. It is, of course, also possible to find combinations of angles such that one peak in the excitation direction coincides with the other peak in the detection direction. Another consideration is the need to choose an energy $\hbar\omega$ such that the QW-RRS signal, $I_e(k, k'; \omega)$, is large. It is apparent from Fig. 2(a) that the averaged QW-RRS spectrum differs significantly from the corresponding exciton absorption spectrum: although they are similar on the low energy side, the high energy tail of the RRS falls off much more rapidly than the absorption. Indeed, the perturbation treatment which is valid for high energies predicts the RRS to fall off as $\sim \omega^{-4}$, compared to ω^{-2} for the absorption.¹⁰ This means that, close to resonance, the MC-RRS will be much stronger for the lower energy polariton feature.

The accuracy of the approximations in the development of the filter model are confirmed by numerical simulations of the MC-RRS process. The simulations use the method introduced in Ref. (5) to calculate specular reflectivity spectra for microcavities. Taking a particular instance of the disorder potential, the evolution of an initial plane wave photon state, of wave vector k , is followed by solving the time-dependent Schrödinger equation for the coupled exciton-photon system. The temporal development of the Rayleigh signal, $G_p(k, k'; t)$, is obtained by calculating the overlap of this state with a plane wave photon of wave vector k' . $G_p(k, k'; t)$ is then transformed into the frequency domain by means of a discrete Fourier transform. Using a similar approach for the bare exciton, it is possible to calculate exact RRS spectra both for the quantum well, as in Fig. 2(a), and for the microcavity, with the same disorder potential in each.

A typical simulated MC-RRS spectrum is shown in Fig. 3(a). It is calculated for the same parameters and an identical disorder potential to the QW-RRS spectrum in Fig. 2(a). Figure 3(b) shows, for comparison, the results of multiplying the QW-RRS spectrum, $I_e(k, k'; \omega)$, of Fig. 2(a) by the microcavity filter functions $|G_p(k; \omega)|^2$, $|G_p(k'; \omega)|^2$, as in Eq.

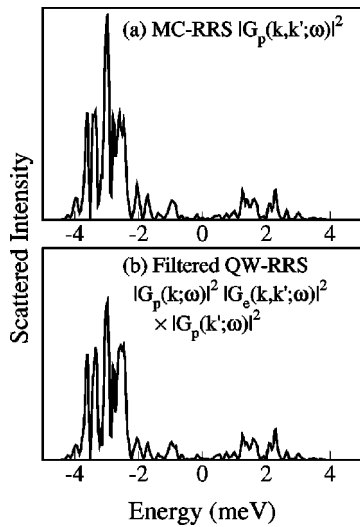


FIG. 3. (a) The calculated microcavity resonant Rayleigh scattering spectrum for the same parameters and disorder potential as Fig. 2. (b) The quantum well resonant Rayleigh scattering spectrum filtered by the microcavity, as in Eq. (3). The parameters for the calculation are given in the caption to Fig. 2.

(3). The two spectra are clearly very similar, with, crucially, the same speckle pattern apparent in each. This comparison with the exact result confirms the accuracy of the filter model in describing MC-RRS. Note that there are some small differences between the spectra, particularly in the heights of the strongest peaks. It is possible that these discrepancies indicate small contributions due to higher order scattering processes, which might be expected to be significant when the first order scattering is strong. However, it is difficult to rule out completely the alternative possibility that the differences are due to numerical errors in the simulations.

MC-RRS has also been discussed by Citrin,¹¹ in connection with scattering experiments which measured a coherent signal in the normal direction after excitation at a finite angle.¹² The formalism of Ref. (11) is similar to the present work, and though quite different approximations have been made, the results derived here should not be considered as contradicting the conclusions of that paper. Indeed, Eq. (4) of Ref. (11) reduces to a form very similar to Eq. (2) of the

present paper, if the term $\Pi_{12}\Pi_{21}$ in the denominator of the polariton Green's function is dropped. This term, when expanded in a power series, leads to some of the multiple scattering processes which have here been shown to be negligible. However, to obtain the filter model, the key approximation that still needs to be made is to equate Π to the off-diagonal exciton Green's function, thereby neglecting all other polariton intermediate states.

There is not yet a great deal of experimental MC-RRS data with which the theory in this paper can be compared. The ideal experiment, measuring RRS from the same QW inside and outside a microcavity, would be hard to perform. As well as the investigations of Norris *et al.* mentioned above,¹² Hayes and co-workers¹³ have measured the detuning dependence of the Rayleigh signal, but discuss it only in the time domain. Most relevant is a very recent paper by Freixanet *et al.*,¹⁴ who performed angular dependent MC-RRS measurements. Their results are in good qualitative agreement with the present work, in that they observe a strong Rayleigh signal round the ring which corresponds to k and k' having the same magnitude. More quantitatively, their expression for the width of this ring is exactly what is implied by the filter theory: if the peak in the filter function has width $\hbar\Gamma$, then the change in k required to lose the overlap of the excitation and detection functions is just $\Delta k = \hbar\Gamma/(dE/dk)$, as in Eq. (1) of Ref. (14).

To conclude, resonant Rayleigh scattering is a phenomenon which requires a theoretical treatment beyond the linear dispersion model of microcavity disorder. However, using a similar approximation of neglecting, as far as possible, disorder scattering between polariton modes leads to an analytic model in which the microcavity acts as a filter for Rayleigh scattering in the quantum well. The accuracy of this model has been confirmed by numerical simulations. The filter model is applicable in the same regime as the linear dispersion model—that is, when the exciton line width is comparable to the vacuum Rabi splitting, a condition which is satisfied in most present day microcavities. In very high quality structures, multiple scattering of polaritons by the disorder will need to be considered. However, like the disorder contribution to the reflectivity line widths, the Rayleigh scattering in such microcavities will be extremely weak.

¹R. Houdré, R.P. Stanley, and M. Ilegems, Phys. Rev. A **53**, 2711 (1996).

²V. Savona and C. Weisbuch, Phys. Rev. B **54**, 10 835 (1996).

³D.M. Whittaker, P. Kinsler, T.A. Fisher, M.S. Skolnick, A. Armitage, A.M. Afshar, M.D. Sturge, and J.S. Roberts, Phys. Rev. Lett. **77**, 4792 (1996).

⁴V. Savona, C. Piermarocchi, A. Quattropani, F. Tassone, and P. Schwendimann, Phys. Rev. Lett. **78**, 4470 (1997).

⁵D.M. Whittaker, Phys. Rev. Lett. **80**, 4791 (1998); D.M. Whittaker, M.S. Skolnick, T.A. Fisher, A. Armitage, D. Baxter, and V.N. Astratov, Phys. Status Solidi A **164**, 13 (1997).

⁶C. Ell, J. Prineas, T.R. Nelson, Jr., S. Park, H.M. Gibbs, G. Khitrova, S.W. Koch, and R. Houdré, Phys. Rev. Lett. **80**, 4795 (1998).

⁷J. Hegarty, M.D. Sturge, C. Weisbuch, A.C. Gossard, and W.

Wiegmann, Phys. Rev. Lett. **49**, 930 (1982).

⁸R. Zimmermann, Nuovo Cimento D **17**, 1625 (1995).

⁹Residual fluctuations due to finite size effects in the simulations are smoothed away by the 0.1 meV of homogeneous broadening.

¹⁰Al.L. Efros, C. Wetzel, and J.M. Worlock, Nuovo Cimento D **17**, 1447 (1995).

¹¹D.S. Citrin, Phys. Rev. B **54**, 16 425 (1996).

¹²T.B. Norris, J.K. Rhee, D.S. Citrin, M. Nishioka, and Y. Arakawa, Nuovo Cimento D **17**, 1295 (1995).

¹³G.R. Hayes, S. Haacke, M. Kauer, R.P. Stanley, R. Houdré, U. Oesterle, and B. Deveaud, Phys. Rev. B **58**, R10 175 (1998).

¹⁴T. Freixanet, B. Sermage, J. Bloch, J.Y. Marzin, and R. Planel, Phys. Rev. B **60**, R8509 (1999).